J|A|C|S
ARTICLES
Published on Web 09/02/2004

Magnetic Circular Dichroism and Cobalt(II) Binding Equilibrium Studies of *Escherichia coli* Methionyl Aminopeptidase

James A. Larrabee,* Chin Hin Leung, Rhonda L. Moore, Thun Thamrong-nawasawat, and Benjamin S. H. Wessler

Contribution from the Department of Chemistry and Biochemistry, Middlebury College, Middlebury, Vermont 05753

Received March 15, 2004; E-mail: larrabee@middlebury.edu

Abstract: Equilibrium dialysis of methionyl aminopeptidase from *Escherichia coli* (*Ec*MetAP) monitored by atomic absorption spectrometry and magnetic circular dichroism (MCD) shows that the enzyme binds up to 1.1 ± 0.1 equiv of Co^{2+} in the metal concentration range likely to be found in vivo. The dissociation constant, K_d, is estimated to be between 2.5 and 4.0 μM. Analysis of the temperature and magnetization behavior of the two major peaks in the MCD spectrum at 495 and 567 nm suggests that these transitions arise from Co^{2+} with different ground states. Ligand field calculations using AOMX are used to assign the 495 nm peak to Co^{2+} in the 6-coordinate binding site and the 567 nm peak to Co^{2+} in the 5-coordinate site. This is further supported by the fact that the binding affinity of the Co^{2+} associated with the 567 nm peak is enhanced when the pH is increased from 7.5 to 9.0, consistent with having an imidazole ligand from a histidine amino acid residue. On the basis of the MCD intensities, it is estimated that, when the 5-coordinate site is fully occupied, 0.1 equiv of cobalt is in the 6-coordinate site. Even when the cobalt concentration is very low, there is a small fraction of binuclear sites in *Ec*MetAP formed through cooperative binding between the 5- and 6-coordinate Co^{2+} ions. The magnetization behavior of the 6-coordinate Co^{2+} MCD peak is consistent with an isolated pseudo-Kramer doublet ground state, suggesting that the cobalt ions in the binuclear sites are not magnetically coupled.

Introduction

Methionyl aminopepdidase (MetAP) catalyzes the hydrolytic removal of N-terminal methionine residues from newly formed proteins. MetAP is just one of a number of metalloaminopeptidases which are essential in protein maturation and degradation processes. This group of enzymes has been the subject of a recent review.[1] MetAP plays a key role in angiogenesis, the growth of new blood vessels, which is necessary for the progression of diseases such as solid tumor cancers and rheumatoid arthritis.[2,3] MetAP has been shown to be the target of two anti-angiogenesis drugs, ovalicin and fumagillin,[4−8] so there has been a large research effort directed at understanding the mechanism of MetAP and how to design effective inhibitors.

Two classes of MetAPs, type 1 and type 2, are found in eukaryotes. Type 2 MetAPs differ from the type 1 MetAPs in that they have an additional insert of amino acid residues in the catalytic domain near the C terminus.[3] Depending on the species, both classes of MetAPs may have an additional N-terminal sequence of 60 or more amino acids. MetAP isolated from *Escherichia coli*, *Ec*MetAP, has a catalytic domain structurally related to the eukaryotic type 1 enzyme, while MetAP isolated from *Pyrococcus furiosus*, *Pf*MetAP, has a catalytic domain structurally related to the type 2 enzyme.[3] Crystal structures of type 2 human MetAP, *Hs*MetAP2 (PDB 1BN5),[8] *Ec*MetAP (PDB 1MAT, 2MAT),[10,11] and *Pf*MetAP (PDB 1XGS)[12] have been reported. Despite the additional catalytic domain inserts found in *Hs*MetAP2 and *Pf*MetAP, the metal binding sites of all three proteins are nearly identical.[1]

The active site for *Ec*MetAP is shown in Figure 1.[11] It contains two metal binding sites indicated by Co(1) and Co(2). Ligands for Co(1) are provided by the imidazole nitrogen of His 171, one oxygen each from the carboxylates side chains of Glu 204, Glu 235, and Asp 108. The ligand set of Co(2) includes one oxygen from each of the carboxylate side chains of Glu 235 and Asp 108 (which bridge the metals) and a bidentate

(1) Lowther, W. T.; Matthews, B. W. *Chem. Rev.* **2002**, *102*, 4581−4607.
(2) Folkman, J. *Nat. Med.* **1995**, *1*, 27−31.
(3) Bradshaw, R. A.; Yi, E. *Essays Biochem.* **2002**, *38*, 65−78.
(4) Taunton, J. *Chem. Biol.* **1997**, *4*, 493−496.
(5) Sin, N.; Meng, L.; Wang, M. Q. W.; Wen, J. J.; Bornmann, W. G.; Crews, C. M. *Proc. Natl. Acad. Sci. U.S.A.* **1997**, *94*, 6099−6103.
(6) Griffith, E. C.; Su, Z.; Turk, B. E.; Chen, S.; Chang, Y.-H.; Wu, Z.; Biemann, K.; Liu, J. O. *Chem. Biol.* **1997**, *4*, 461−471.
(7) Lowther, W. T.; McMillen, D. A.; Orville, A. M.; Matthews, B. W. *Proc. Natl. Acad. Sci. U.S.A.* **1998**, *95*, 12153−12157.
(8) Liu, S.; Widom, J.; Kemp, C. W.; Crews, C. M.; Clardy, J. *Science* **1998**, *282*, 1324−1327.
(9) Arfin, S. M.; Kendall, R. L.; Hall, L.; Weaver, L. H.; Stewart, A. E.; Matthews, B. W.; Bradshaw, R. A. *Proc. Natl. Acad. Sci. U.S.A.* **1995**, *92*, 7714−7718.
(10) Roderick, S. L.; Matthews, B. W. *Biochemistry* **1993**, *32*, 3907−3912.
(11) Lowther, W. T.; Orville, A. M.; Madden, D. T.; Lim, S.; Rich, D. H.; Matthews, B. W. *Biochemistry* **1999**, *38*, 7678−7688.
(12) Tahirov, T. H.; Oki, H.; Tsukihara, T.; Ogasahara, K.; Yutani, K.; Ogata, K.; Izu, Y.; Tsunasawa, S.; Kato, I. *J. Mol. Biol.* **1998**, *284*, 101−124.

10.1021/ja0485006 CCC: $27.50

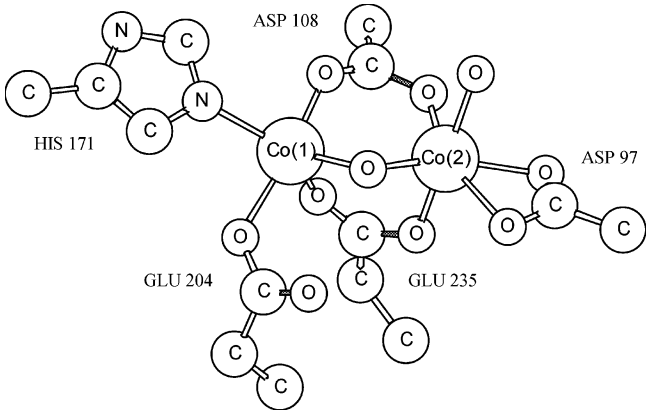

Figure 1. Active site structure of *Ec*MetAP as taken from ref 11 (PDB 2MAT). Only the amino acid side chains that serve as ligands to the metals are shown, and only the waters (or hydroxides) that are bound to the metals are shown. Hydrogen atoms are not shown. Reprinted from ref 11. Copyright 1999 American Chemical Society.

carboxylate side chain from Asp 97. In both the *Ec*MetAP and *Pf*MetAP crystal structures a bridging water or hydroxide is found, giving Co(1) a fifth ligand.[11,12] In the *Ec*MetAP structure a water ligand is found for Co(2), making it 6-coordinate.

All three structures are reported with two cobalt ions occupying the Co(1) and Co(2) sites, and all MetAPs isolated so far are active with Co^{2+}.[1,3] The combination of these observations led many to assume that all MetAPs contained a binuclear cobalt active site in vivo. However, these MetAPs were isolated in the apo form, and cobalt was introduced into the protein in vitro. Recently, cobalt as the physiologically relevant metal has been challenged. Arguments have been made in support of Zn^{2+} as the in vivo metal for yeast MetAP,[13,14] and of Fe^{2+} as the in vivo metal for *Ec*MetAP.[15−17] Part of the argument against cobalt is based on the fact that it is much rarer in cellular media than either zinc or iron. Isolation of the bimetallic prolidase from *P. furiosus* with a bound cobalt ion has been reported, raising the possibility that the in vivo metal for *Pf*MetAP could also be cobalt.[18] It has been suggested that the in vivo metal is determined by ambient levels of metal in the organism, and may even vary within a species depending upon local environmental conditions.[3,19,20] While specific activity is dependent on which metal occupies the Co(1) and Co(2) sites, there is no evidence that the mechanism of active MetAPs varies with the type of metal.

Recently, it has been proposed that *Ec*MetAP and *Pf*MetAP are monometallic hydrolases in vivo.[15,17,21] This conclusion was based on experimental evidence including activity titrations, calorimetry titrations, EPR, NMR, and EXAFS. It was determined that these enzymes reached a maximum in specific activity when 1 equiv of Co^{2+} was added. NMR and EXAFS were employed to show that the high-affinity metal binding site is Co(1). The dissociation constants, K_d, of Co(1) and Co(2) were estimated by activity titration to be 0.3 ± 0.2 μM and 2.5 ± 0.5 mM, respectively, in *Ec*MetAP.[15] Similarly, the dissociation constants for Co(1) and Co(2) were estimated to be 0.05 ± 0.015 μM and 0.35 ± 0.02 mM, respectively, in *Pf*MetAP.[21] It was argued that, with such a large difference in metal binding affinity, only the Co(1) site would be occupied at physiological metal ion concentrations.

Crystal structures of *Hs*MetAP complexed with a natural angiogenesis inhibitor, fumagillin (PDB 1BOA), and two synthetic analogues, ovalicin (PDB 1B59) and TNP 470 (PDB 1B6A), show interactions (not necessarily bonds but closer than the van der Waals radii) of the bound inhibitors with both Co(1) and Co(2).[8] It has been proposed that the fumagillin complex with *Ec*MetAP is similar.[7] Likewise, a structure of *Ec*MetAP complexed with a bestatin-based inhibitor shows that the inhibitor is bound to both cobalts.[22] A number of other complexes of transition-state analogues and reaction products with *Ec*MetAP show interactions with both metals.[22]

There is other evidence in addition to the crystal structures that *Ec*MetAP is a bimetallic hydrolase. One study reports a $[Co^{2+}]$/[protein] ratio of 1.6 when wild-type *Ec*MetAP is isolated from the growth medium with no added cobalt. When any of the Co(1) or Co(2) amino acid ligands are replaced by amino acids with side chains that cannot function as metal ligands, the resulting mutant *Ec*MetAP isolated from the medium has no bound cobalt.[23] A kinetic study of different metals and substrates on *Hs*MetAP concluded that two metals were necessary for full activity;[24] however, this conclusion has been refuted.[21]

While the type of metal may not be crucial to reach an understanding of how MetAPs function, the number of metals in the active site almost certainly will be important for a mechanistic understanding. The search for new and more potent MetAP inhibitors as possible anti-angiogenesis drugs should be influenced by knowing whether MetAP is a monometallic or bimetallic enzyme under physiological conditions. Over the course of our magnetic circular dichroism (MCD) study of *Ec*MetAP, we attempted to prepare samples for MCD which contained only a single Co^{2+} in the Co(1) site. When we added 1 equiv of Co^{2+} to *Ec*MetAP, we reproduced the published electronic absorption spectrum, but the MCD spectrum could not be interpreted with only a single type of Co^{2+}. Even in preparations in which the $[Co^{2+}]$/[protein] ratio was less than 1, the MCD spectrum could not be understood in terms of only a single type of Co^{2+}. This led us to reexamine the Co^{2+} binding equilibrium with *Ec*MetAP using anaerobic equilibrium dialysis monitored by MCD and atomic absorption (AA) spectrometry. We have also assigned the electronic absorption and MCD spectra using ligand field calculations based on the angle overlap method (AOM).

(13) Walker, K. W.; Bradshaw, R. A. *Protein Sci.* **1998**, *7*, 2684−2687.
(14) Walker, K. W.; Bradshaw, R. A. *J. Biol. Chem.* **1999**, *274*, 13403−13409.
(15) (a) D'souza, V. M.; Bennett, B.; Copik, A. J.; Holz, R. C. *Biochemistry* **2000**, *39*, 3817−3826. (b) Copik, A. J.; Swierczek, S. I.; Lowther, W. T.; D'souza, V. M.; Matthews, B. M.; Holz, R. C. *Biochemistry* **2003**, *42*, 6283−6292. (c) Bennett, B.; Antholine, W. E.; D'souza, V. M.; Chen, G.; Ustinyuk, L.; Holz, R. C. *J. Am. Chem. Soc.* **2002**, 13025-13034. (d) D'souza, V. M.; Swierczek, S. I.; Cosper, N. J.; Meng, L.; Ruebush, S.; Copik, A. J.; Scott, R. A.; Holz, R. C. *Biochemistry* **2002**, *41*, 13096−13105.
(16) D'souza, V. M.; Holz, R. C. *Biochemistry* **1999**, *38*, 11079−11085.
(17) Cosper, N. J.; D'souza, V. M.; Scott, R. A.; Holz, R. C. *Biochemistry* **2001**, *40*, 13302−13309.
(18) Ghosh, M.; Grunden, A. M.; Dunn, D. M.; Weiss, R.; Adams, M. W. W. *J. Bacteriol.* **1998**, *180*, 4781−4789.
(19) Kobayashi, M.; Shimizu, S. *Eur. J. Biochem.* **1999**, *261*, 1−9.
(20) Lowther, W. T.; Matthews, B. W. *Biochim. Biophys. Acta* **2000**, *1477*, 157−167.
(21) Meng, L.; Ruebush, S.; D'souza, V. M.; Copik, A. J.; Tsunasawa, S.; Holz, R. C. *Biochemistry* **2002**, *41*, 7199−7208.
(22) Lowther, W. T.; Zhang, Y.; Sampson, P. B.; Honek, J. F.; Matthews, B. W. *Biochemistry* **1999**, *38*, 14810−14819.
(23) Chiu, C.-H.; Lee, C.-Z.; Lin, K.-S.; Tam, M. F.; Lin, L.-Y. *J. Bacteriol.* **1999**, *181*, 4686−4689.
(24) Yang, G.; Kirkpatrick, R. B.; Ho, T.; Zhang, G.-F.; Liang, P.-H.; Johanson, K. O.; Casper, D. J.; Doyle, M. L.; Marino, J. P.; Thompson, S. K.; Chen, W.; Tew, D. G.; Meek, T. D. *Biochemistry* **2001**, *40*, 10645−10654.

Materials and Methods

Enzyme Purification. A starter culture of the modified *E. coli* was kindly provided by Professor W. Todd Lowther, Department of Biochemistry, Wake Forest University of Medicine. *Ec*MetAP was overexpressed and purified according to a published method except Co^{2+} was excluded from the elution buffer in the final Superdex 75 Hi load column chromatography step.[7] We noted, as have others, that *Ec*MetAP is sensitive to aggregation/precipitation induced by divalent metals. All water used was first purified by reverse osmosis and then passed through a Hydro Picotech 2 purifier that included columns to remove carbonaceous materials and metals. This polished water had no detectable levels of Mn, Fe, Co, Ni, Cu, or Zn by graphite furnace AA. Nevertheless, as an added precaution, all buffers used in the final steps of the purification (after the six-His tag was removed) were treated with Chelex 100 resin (Bio-Rad).[16] Protein concentrations were estimated by absorbance at 280 nm using an extinction coefficient of 16350 M^{-1} cm^{-1}.[7] Activity was measured as previously described using the tetrapeptide MetGlyMetMet (Sigma) as substrate.[25] As a precaution against oxidation, 15 mM methionine was added to all buffers during the purification steps. This methionine was removed by anaerobic dialysis versus 25 mM HEPES (Sigma) buffer, pH 7.5, containing 150 mM KCl using a 10000 MWCO Slide-A-Lyzer (Pierce) dialysis cassette. Removal of the methionine is essential before any optical measurements as Co^{2+} forms a complex with methionine having an absorption maximum at 540 nm ($\epsilon = 65$ M^{-1} cm^{-1}, assuming that the reaction between 1 mM Co^{2+} and 15 mM methionine goes to completion at pH 7.5 to form 1 mmol of complex).

Anaerobic Dialysis. All handling of *Ec*MetAP after methionine was removed was done anaerobically. Dialysis of cobalt into or out of enzyme solutions is accomplished using either 0.5 or 3.0 mL 10000 MWCO Slide-A-Lyzer dialysis cassettes (Pierce). Large volumes of buffer were first degassed by He sparging, and then smaller volumes of the degassed buffer were frozen and placed under vacuum during transfer into the glovebox while they thawed. Enzyme was loaded into the dialysis cassettes in the glovebox and placed into 200 mL of degassed buffer in a 250 mL Kontes jacketed reaction beaker. Coolant from an external bath was circulated through the reaction beaker jacket to keep the dialysis buffer and enzyme at 4 °C.

Physical Measurements. Absorption spectra were recorded on a Cary 6000i UV/vis/near-infrared absorption spectrometer. Cobalt was determined on a Perkin-Elmer 4110 ZL graphite furnace atomic absorption spectrometer with Zeeman background correction. The AA method was set at the manufacturer's recommended conditions for cobalt at 242.5 nm. The instrument was calibrated between 0 and 40 ppb cobalt using a standard of 99.999% pure $CoCl_2 \cdot 6H_2O$ (Janssen Chimica) dissolved in 0.2% trace metal grade nitric acid (Fisher). Enzyme samples were diluted with buffer to bring them into the calibration range. Buffer was used as the blank, but cobalt in the buffer was not detected. MCD spectra were recorded at 2 nm bandwidth on a JASCO J-600 spectropolarimeter equipped with an Oxford SM-4 magnet/cryostat with an Oxford ITC-4 temperature controller. Temperatures were measured with a Lake Shore Cryogenics carbon/glass resistor calibrated between 1.45 and 99.99 K and located 2 mm from the sample. Samples were mixed with degassed glycerol (99.5%, Sigma-Aldrich) in a ratio of 1 part protein in buffer to 2 parts glycerol (v/v), and placed in a 0.62 cm path length brass cell with quartz windows. The zero-field spectrum was subtracted as a baseline as well as a dialysis buffer blank. The latter had a small contribution near 500 nm from free Co^{2+} added to the equilibrium dialysis buffer. Details of variable-temperature variable-field (VTVH) MCD data collection have been previously published.[26] MCD spectra were fit to the minimum number of Gaussian peaks using GRAMS/AI software (Thermo Electron Corp.). The heights of the Gaussian peaks were used for quantitative calculations.

AOM Calculations. Angular overlap method calculations were made using AOMX, a program based on routines developed by Hoggard for d^3 transition-metal ions and extended to d^n systems by Adamsky.[27] AOMX determines the optimum ligand field parameters needed to fit an observed set of d−d transitions based on a given structure. Co(1) and Co(2) were treated separately. Input to AOMX requires the ligand coordinates (polar r, θ, φ or Cartesian x, y, z) assuming that the metal is at 0, 0, 0. The latest PDB structure for *Ec*MetAP, 2MAT, was used to create a file containing only the active site metals and their ligands using RASMOL. This abbreviated file was then exported to CS ChemDraw 3D. In ChemDraw 3D, each metal was in turn set at the origin and the Cartesian coordinates of the ligand atoms were generated. AOMX outputs the polar coordinates when given the Cartesian coordinates, so a check against the metal−ligand bond distances (easily obtained from RASMOL) is used to confirm that there are no errors in the coordinate input. The Co(1) ligand set includes the imidazole nitrogen from His 171 at 2.15 Å, a bridging carboxylate oxygen from Asp 108 at 1.91 Å, a carboxylate oxygen from Glu 204 at 2.08 Å, a bridging carboxylate oxygen from Glu 235 at 1.99 Å, and an oxygen from a bridging hydroxide or water at 2.14 Å. The Co(2) ligand set includes two oxygens in a bidentate carboxylate from Asp 97 at 2.13 and 2.37 Å, a bridging carboxylate oxygen from Asp 108 at 2.04 Å, a bridging carboxylate oxygen from Gsu 235 at 2.15 Å, an oxygen from the bridging hydroxide/water at 2.08 Å, and a water oxygen at 2.20 Å. AOMX does not use the bond distances to fit the spectrum; only the bond angles are important (and are fixed at those given by the crystal structure), but the bond distances are reflected by the magnitude of the resulting ligand field parameters, ϵ_σ and ϵ_π.[26]

Results

MCD Spectrum and Analysis. Figure 2 shows the MCD and absorption spectra of *Ec*MetAP having 0.8 equiv of Co^{2+}/mol of protein. The protein samples were prepared by anaerobic dialysis versus buffer containing 20 μM Co^{2+}. The absorption spectrum is nearly identical with that previously published for *Ec*MetAP with [Co]/[MetAP] = 1, but the molar absorptivities, based on protein concentration, are about 20% lower than those reported due to the fact that the protein has only 0.8 equiv of bound cobalt.[15a] Four peaks, counting a weak shoulder between 490 and 540 nm centered at about at 526 nm, were observed in the visible region at 685, 629, 571, and 526 nm. The MCD spectrum in Figure 2 has three of the same four peaks (some blue shifted because of the low temperature), but remarkably the MCD is dominated by the peak at 495 nm. There is an additional feature at 472 nm. The MCD bands at 472, 495, 567, and 625 nm are temperature-dependent and thus are C terms associated with the paramagnetic Co^{2+}.[28] There is a weak, temperature-independent, A term near 408 nm that is associated with aromatic residues in the protein. In more concentrated samples of *Ec*MetAP an additional weak MCD peak is observed at 679 nm.

(25) Larrabee, J. A.; Thamrong-nawasawat, T.; Mon, S. Y. *Anal. Biochem.* **1999**, *269*, 194−198.
(26) Larrabee, J. A.; Alessi, C. M.; Asiedu, E. T.; Cook, J. O.; Hoerning, K. R.; Klingler, L. J.; Okin, G. S.; Santee, S. S.; Volkert, T. L. *J. Am. Chem. Soc.* **1997**, *119*, 4182−4196.
(27) Hoggard, P. E. *Topics in Current Chemistry*; Springer-Verlag: Berlin, 1994; Vol. 171, pp 113−141. The AOMX program is maintained by H. Adamsky, Institut fur Theoretische Chemie, Heinrich Heine Universitat, Duesseldorf, Germany, e-mail adamsky@theochem.uni-duesseldorf.de. The program can also be run on the Web using the AOMX server at http://www.theochem.uni-duesseldorf.de/users/heribert/aomx/start.main.html.
(28) (a) Johnson, M. K. In *Physical Methods in Bioinorganic Chemistry*; Que, L., Ed.; University Science Books: Sausalito, CA, 2000; Chapter 5. (b) Krzystek, J.; Zvyagin, S. A.; Ozarowski, A.; Fiedler, A. T.; Brunold, T. C.; Telser, J. *J. Am. Chem. Soc.* **2004**, *126*, 2148−2155.

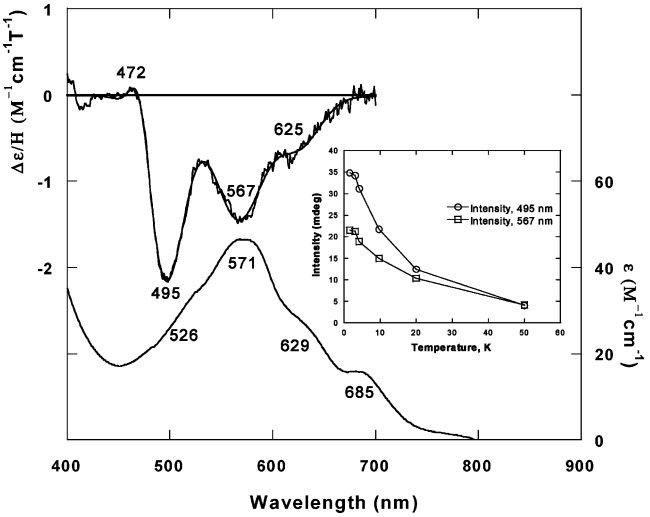

Figure 2. MCD (top) and electronic absorption (bottom) spectra of *Ec*MetAP in 25 mM HEPES, 150 mm KCl buffer at pH 7.5. Cobalt was introduced by anaerobic dialysis versus 20 μM Co^{2+}. The MCD spectrum was recorded at 1.6 K at a magnetic field of 3.5 T on a sample 0.3 mM in protein. The bound cobalt to protein ratio was determined to be 0.8 by AA. Superimposed on the MCD spectrum is the best fit of the data to four Gaussian peaks after peak deconvolution. The absorption spectrum was recorded at room temperature versus the dialysis buffer on the same sample but without added glycerol (0.9 mM). A 0.9 mM apo-*Ec*MetAP spectrum was subtracted as a baseline. The inset is a plot of the 495 and 567 nm MCD peak intensities versus temperature at 3.5 T. Both $\Delta\epsilon/\mathbf{H}$ and ϵ scales are based on protein concentration.

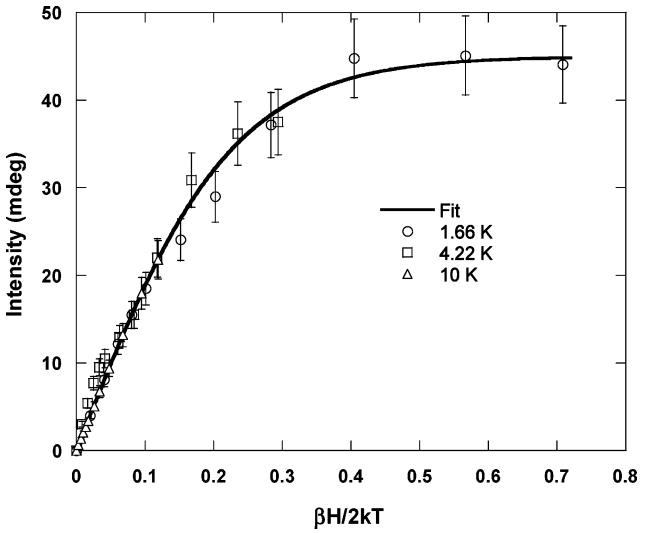

Figure 3. Magnetization plot of the 495 nm MCD band from the sample used in Figure 2. Data were collected at 1.66, 4.22, and 10 K and magnetic fields between 0 and 3.5 T. The line is the best fit to eq 1 with $g = 4.45$, $I = 45.0$, and $B = 0$.

The combination of the number and energy of peaks in the MCD and absorption spectra makes it difficult to attribute them all to a single type of Co^{2+}. The inset of Figure 2 shows the MCD intensities of the 495 and 567 nm bands at a fixed magnetic field of 3.5 T plotted against temperature. As the temperature is raised from 1.6 to 50 K, the intensities decrease, as they should for C terms; however, the decrease is more rapid for the 495 nm peak than for the 567 nm peak. In variable-temperature MCD (at fixed field) the intensity change is a property of the ground state; therefore, this intensity behavior suggests that the 495 and 567 nm MCD bands arise from two different ground states, implying two different types of Co^{2+}

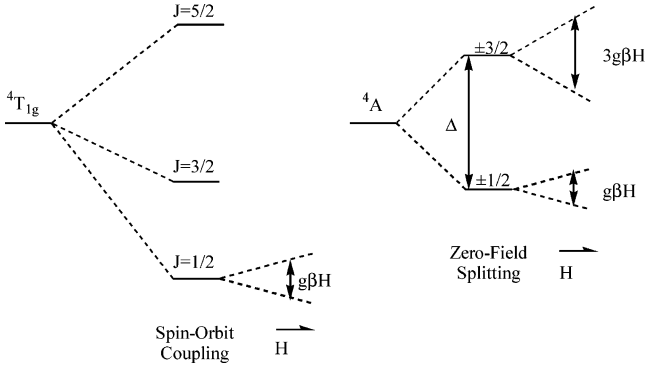

Figure 4. Idealized schemes for ground-state splitting in 6- and 5-coordinate Co^{2+}. The left diagram is for an octahedral ground state. The dominant zero-field splitting is due to in-state spin−orbit coupling. If $\zeta = 450$ cm^{-1}, then the difference between the $J = 1/2$ and $J = 3/2$ levels would be 225 cm^{-1}; thus, only the $J = 1/2$, "pseudo-Kramer doublet" would be populated at low temperatures. The right diagram is applicable to either of the two idealized 5-coordinate geometries, D_{3h} or C_{4v}, because the ground state is ^4A in both cases. In 5-coordinate geometry the zero-field splitting, Δ, is small because any spin−orbit coupling must involve a higher energy ^4E term. MCD intensity can arise simultaneously from the $\pm 3/2$ and $\pm 1/2$ levels, causing a complex magnetization curve. At high magnetic fields, the $\pm 3/2$ and $\pm 1/2$ levels will mix.[28b] The figure is drawn for a positive Δ. A negative Δ would have the $\pm 3/2$ level lower than the $\pm 1/2$ level.

ions.[26,28] The possibility that the 495 and 567 nm peaks arise from Co^{2+} in the Co(2) and Co(1) sites, respectively, was further explored.

A more detailed way to look at ground states is to compare magnetization plots. Figure 3 shows the plot of the low-temperature MCD intensity of the 495 nm peak versus $\beta\mathbf{H}/2kT$. The agreement in MCD intensities having the same value of $\beta\mathbf{H}/2kT$ but obtained at three different temperatures is an indication that the transition arises from a simple Kramer doublet.[28a] This at first may seem unlikely as octahedral Co^{2+} has a $^4T_{1g}$ ground state; however, the $^4T_{1g}$ ground state is subject to strong in-state spin−orbit coupling which leads to a large zero-field splitting (>100 cm^{-1}).[26,29] The large zero-field splitting creates a pseudo-Kramer doublet ground state that can be treated as an isolated Kramer doublet in the low-temperature regime (Figure 4). The low-temperature MCD magnetization data from the 495 nm band were fit to a simple tanh function as given in eq 1,[28a] where $\Delta\epsilon$ is the MCD intensity, I is a

$$\Delta\epsilon = I \tanh\left(\frac{g\beta\mathbf{H}}{2kT}\right) + B\mathbf{H} \qquad (1)$$

constant, g is the isotropic g factor, β is the Bohr magneton, $\mathbf{H}$ is the magnetic field, k is Boltmann's constant, T is the absolute temperature, and B is the temperature-independent B term intensity. The fit shown in Figure 3 was made with $I = 45.0$, $g = 4.45$, and $B = 0$. A value of 4.4 is typical for isotropic g values for high-spin, 6-coordinate Co^{2+}.[29,30]

The magnetization curves for the 567 nm peak are shown in Figure 5 at three different temperatures. These curves are very different from the curve for the 495 nm band. The 567 nm band curves do not approach saturation, which is evidence that they have a temperature-dependent B term component.[28] Furthermore, the 567 nm band curves are strongly "nested", which is

(29) Figgis, B. N. *Introduction to Ligand Fields*; Interscience: New York, 1966; Chapter 11.
(30) Parish, R. V. *NMR, NQR, EPR, and Mossbauer Spectroscopy in Inorganic Chemistry*; Ellis Horwood: New York, 1990; p 193.

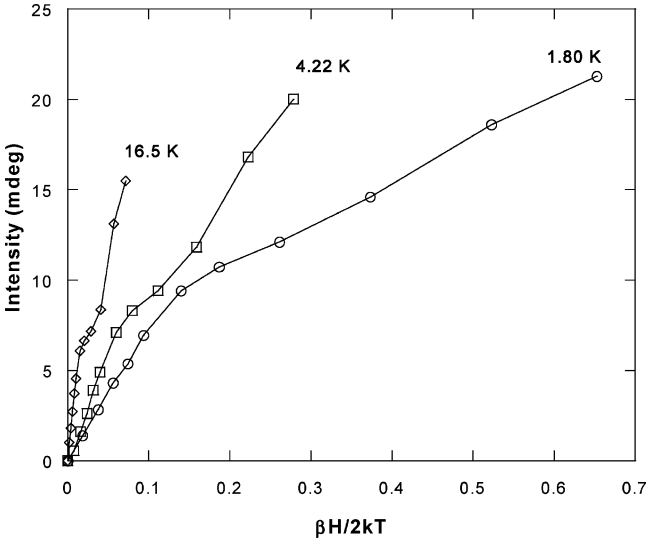

Figure 5. Magnetization plot of the 567 nm MCD band from the sample used for Figure 2.

typical for $S > 1/2$ spin systems in which there is a low-lying excited state that can be populated at the experimental temperatures.[28] Five-coordinate Co^{2+} can exhibit zero-field splitting (ZFS) which splits $\pm 1/2$ and $\pm 3/2$ spins of the ^4A ground state by Δ (Figure 4). Fits of the low-field variable-temperature MCD data from the 567 nm band to eq 2 yield an estimate for the absolute value of Δ of 10 ± 5 cm^{-1} for the ZFS.[26]

$$\text{intensity} = \sum_i \left(\frac{C_i}{kT} \alpha_i \mathbf{H} + B_i \alpha_i \mathbf{H} \right) \qquad (2)$$

where

$$\alpha_1 = \frac{1}{1 + e^{-\Delta}/kT}$$

and

$$\alpha_2 = \frac{e^{-\Delta}/kT}{1 + e^{-\Delta}/kT}$$

The magnetization curves for the 495 and 567 nm peaks explain why the MCD intensities for the 495 and 567 nm bands drop at a different rate with increasing temperature (inset of Figure 2). Population of the low-lying $\pm 3/2$ state (or $\pm 1/2$ state if the sign of Δ is negative) increases as the temperature is raised, and since this state could have more intrinsic MCD intensity, the peaks associated with the 5-coordinate Co^{2+} decrease in intensity less rapidly than those peaks associated with 6-coordinate Co^{2+}. A further complication in the magnetization curve for 5-coordinate Co^{2+} is the possibility of field-induced mixing of the $\pm 1/2$ and the $\pm 3/2$ states.[28] The magnetization curves for the 495 and 567 nm bands are strong evidence that these two transitions arise from two different ground states. The fit of the VTVH MCD data to a simple Kramer doublet model suggests that there is no low-lying excited state and that the 495 nm transition arises from 6-coordinate Co^{2+}.

AOMX Analysis. The strong negative band at 495 nm and weaker band at 472 nm are very similar in energy to those of MCD spectra reported for a variety of 6-coordinate Co^{2+} complexes.[31] The MCD bands at 567, 625, and 679 nm are consistent in energy and pattern with 5-coordinate Co^{2+} complexes.[26,31] The MCD transition energies at 567, 625, and 679 nm were fit to a 5-coordinate Co^{2+} ion having the same ligand set and geometry as Co(1) using the angular overlap method, AOMX.[27] Table 1 gives the results of the AOMX fits.

Of the five ligands to Co(1) in *Ec*MetAP, only the imidazole nitrogen can be considered a strong-field ligand, and it is at a relatively long 2.15 Å. The remaining four ligands are made up from weaker field carboxylate oxygen and water (or hydroxide) ligands. Two of these (the bridging hydroxide/water and the carboxylate oxygen from Glu 204) are at about 2.1 Å.

Table 1. Summary of AOMX Calculations[a]

		d–d transition, nm	
	origin in D_{3h}	obsd	calcd
5-coord Co(1) site	$^4A_2 \rightarrow {}^4A_2(P)$	679	666
	$^4A_2 \rightarrow {}^4E(P)$	625	612
	$^4A_2 \rightarrow {}^4E(P)$	567	557
		d–d transition, nm	
	origin in O_h	obsd	calcd
6-coord Co(2) site	$^4T_{1g} \rightarrow {}^4T_{1g}(P)$	495	495
	$^4T_{1g} \rightarrow {}^2A_{1g}(P)$	472	472

[a] AOMX parameters (cm^{-1}): 5-coordinate Co(1), ϵ_σ(His 171) = 4790, ϵ_σ(OH or H_2O) = 1490, ϵ_σ(Glu 235) = 2820, ϵ_σ(Glu 204) = 2260, ϵ_σ(Asp 108) = 2820, B = 740, C = 3400; 6-coordinate Co(2), ϵ_σ(bridge OH or H_2O) = 3040, ϵ_σ(H_2O) = 3800, ϵ_σ(Glu 235) = 3460, ϵ_σ(Asp 97 long) = 2760, ϵ_σ(Asp 97 short) = 3460, ϵ_σ(Asp 108) = 3460, B = 850, C = 3910.

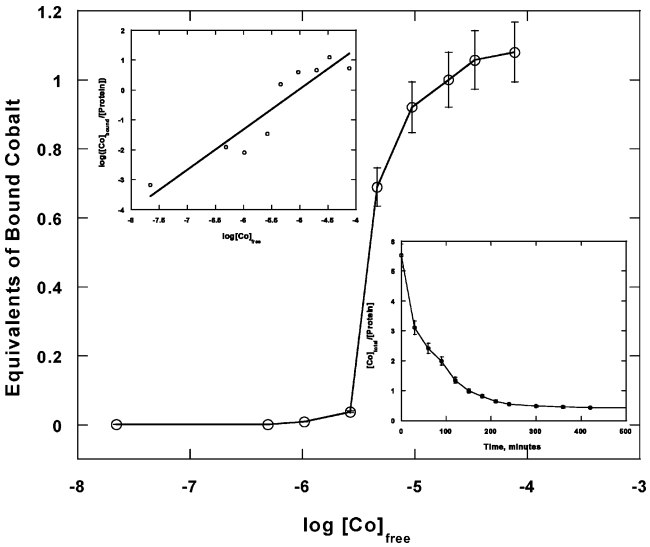

Figure 6. Co^{2+} binding to *Ec*MetAP. [*Ec*MetAP] was 0.1 mM in 25 mM pH 7.5 HEPES with 150 mM KCl. After each addition of Co^{2+} to the dialysis buffer the dialysis was allowed to equilibrate for 48 h. Then a sample was removed from the buffer and from the dialysis cassette, and total [Co] was determined for both. Total [protein] was determined for the cassette sample. $[Co]_{bound}$ was determined by difference. Above 80 μM, the precision of the cobalt determination was no longer good enough to measure a difference between protein solution and buffer solution. The inset to the upper left shows the Hill plot of the data according to eq 3. The Hill plot has a slope of 1.3 and an intercept of 6.7. The inset to the lower right shows the removal of total cobalt as a function of time. The sample was a 0.1 mM *Ec*MetAP sample anaerobically dialyzed versus 0.5 mM Co^{2+} for 48 h. The sample was then dialyzed versus metal-free buffer. Samples were removed from the dialysis cassette for cobalt determination by AA and protein determination. The metal-free buffer was changed every 3 h.

(31) Kaden, T. A.; Holmquist, B.; Vallee, B. L. *Inorg. Chem.* **1974**, *13*, 2585−2590.

With this ligand set it is not possible to get spin-allowed d−d transitions as high in energy as 495 nm from a 5-coordinate Co^{2+} complex.[26] We attempted to fit the 495 nm band to the 5-coordinate Co(1) and could not without allowing ϵ_σ(N) to exceed 6150 cm^{-1} and ϵ_σ(bridging OH or H_2O) to exceed 5500 cm^{-1}, values way in excess of even very strong field ligands in other 5-coordinate Co^{2+} complexes.[26] The 495 nm band can be fit to a 6-coordinate Co^{2+} having the geometry of Co(2).

Equilibrium Dialysis Monitored by AA. The MCD and AOMX results show that both 5- and 6-coordinate Co^{2+} exist in *Ec*MetAP even when [Co^{2+}] is 20 μM (7 μM after dilution with glycerol). This is well below the reported concentration necessary to bind a second equivalent of Co^{2+}. According to this report the dissociation constant for the second equivalent of Co^{2+} is 2.5 mM.[15a] Figure 6 shows the results of an anaerobic equilibrium dialysis experiment on a 0.1 mM *Ec*MetAP sample monitored by atomic absorption. The ratio of bound cobalt to total protein is plotted as a function of [Co^{2+}] in the dialysis buffer, and it appears that the bound cobalt is approaching 1.1 equiv/equiv of protein at the limit of 80 μM Co^{2+}. The data were reworked into a Hill plot (shown in the inset) according to the following scheme of equations:[32,33]

$$n\mathrm{Co}^{2+} + \mathrm{MetAP} \rightleftarrows \mathrm{Co}_n\mathrm{MetAP}$$

$$K = \frac{[\mathrm{Co}_n\mathrm{MetAP}]}{[\mathrm{Co}^{2+}]^n[\mathrm{MetAP}]}$$

$$\log \frac{[\mathrm{Co}_n\mathrm{MetAP}]}{[\mathrm{MetAP}]} = n \log [\mathrm{Co}^{2+}] + \log K \qquad (3)$$

The best-fit line to the Hill plot has a slope of $n = 1.3 \pm 0.2$ and an intercept of 6.7 ± 0.4. This corresponds to a dissociation constant of 0.2 μM (error range 0.07−0.5), which agrees with another study which found a $K_d = 0.3 \pm 0.2$ μM by an activity titration.[15a] In Figure 6, the concentration of Co^{2+} corresponding to $[Co]_{bound}/[protein] = 0.5$ is 4 μM, which equals K_d assuming that only a single cobalt binds ($n = 1.0$ in eq 3). The experiment was repeated at a higher initial *Ec*MetAP concentration of 1 mM with similar results (vide infra).

A sample of *Ec*MetAP was dialyzed versus 0.5 mM Co^{2+} and then dialyzed versus metal-free buffer (lower right inset of Figure 6). The initial total cobalt/protein ratio was about 6. The amount of bound cobalt was unknown, but from a later experiment (Figure 8) it can be assumed that there are at least 2 equiv of bound Co^{2+}. After exhaustive dialysis most of the cobalt was removed; however, a small fraction, about 20%, remained resistant to removal, even after 140 h of dialysis versus metal-free buffer. Dialysis versus metal-free buffer for 3 h results in about 1 equiv of cobalt per protein, similar to what others have reported,[15] but no leveling off of the curve was observed at this point to indicate any resistance to removal.

Equilibrium Dialysis Monitored by MCD and AA. At concentrations of Co^{2+} below 100 μM 1.1 ± 0.1 equiv of cobalt binds to *Ec*MetAP; however, it also appears that the Co^{2+} exists

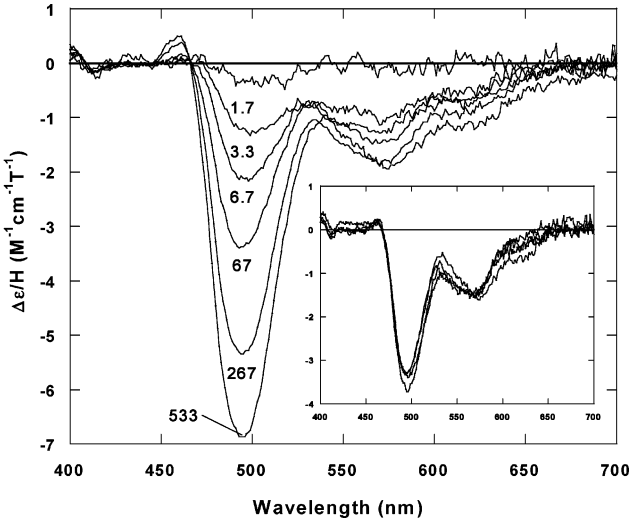

Figure 7. MCD spectra of *Ec*MetAP in 25 mM HEPES, 150 mM KCl, pH 7.5. Cobalt was introduced by anaerobic dialysis. The main figure is for samples obtained with 5, 10, 20, 200, 800, and 1600 μM Co^{2+} in the dialysis buffer. All MCD spectra were recorded at 1.6 K and 3.5 T with the sample mixed 1/3 with glycerol (thus, the final Co^{2+} concentrations are 1.7, 3.3, 6.7, 67, 267, and 533 μM as marked on the spectra). The inset shows the MCD spectra of samples prepared with 40, 80, 160, and 200 μM Co^{2+} in the dialysis buffer. This is the range of [Co^{2+}] in which the 495 and 567 nm peak intensities remain nearly constant.

in both 6- and 5-coordinate forms. To probe further the nature of Co^{2+} binding to *Ec*MetAP, the equilibrium dialysis experiment was repeated using 1.0 mM *Ec*MetAP, samples were removed at each [Co^{2+}], and an MCD spectrum was taken. After the MCD, protein concentration was determined by absorbance at 280 nm and total cobalt was determined by AA. Free [Co^{2+}] was calculated from what was added to the dialysis buffer and the glycerol dilution factor (1/3). The MCD spectra are shown in Figures 7 and 9, and the overall results are summarized in Figure 8.

The MCD peaks associated with 5- and 6-coordinate Co^{2+} increase steadily and at the same rate until the free [Co^{2+}] in the dialysis buffer reaches 40 μM (13 μM free Co^{2+} after dilution with glycerol). At this point the *Ec*MetAP sample had 1.1 ± 0.1 equiv of bound cobalt as determined by AA. As the [Co^{2+}] is increased in the dialysis medium up to 200 μM, there is very little increase in MCD peak intensities at 495 or 567 nm (inset of Figure 7). Likewise, the total bound cobalt as determined by AA shows little increase in this range (Figure 8). If the data for total bound cobalt (below 67 μM free Co^{2+}) are treated to a Hill plot analysis, the slope is found to be 1.3. When the [Co^{2+}] is increased above 200 μM, the intensity at 495 nm begins to increase, but the 5-coordinate peak at 567 nm stays constant. This behavior continues until the [Co^{2+}] reaches 1600 μM, above which *Ec*MetAP (at 1 mM) begins to aggregate and the experiment is terminated.

This series of MCD and AA experiments afforded the possibility of determining values for $\Delta\epsilon_{567}/\mathbf{H}$ and $\Delta\epsilon_{495}/\mathbf{H}$ based on equivalents of bound cobalt. At the point in the equilibrium dialysis experiment that the 567 nm MCD peak saturates, we can assume that the 5-coordinate site is fully occupied. This yields a value for $\Delta\epsilon_{567}/\mathbf{H} = 1.9 \pm 0.2$ M^{-1} cm^{-1} T^{-1}. This constant then is used to determine the number of equivalents of bound 5-coordinate Co^{2+}, and with the total bound cobalt determined by AA, the difference gives a value for the

(32) (a) van Holde, K. E.; Johnson, W. C.; Ho, P. S. *Principles of Physical Biochemistry*; Prentice Hall: Upper Saddle River, NJ, 1998; Chapter 15. (b) Marshall, A. G. *Biophysical Chemistry: Principles, Techniques, and Applications*; Wiley: New York, 1978; pp 70−84.
(33) Dutton, T. J.; Baumann, T. F.; Larrabee, J. A. *Inorg. Chem.* **1990**, *29*, 2272−2278.

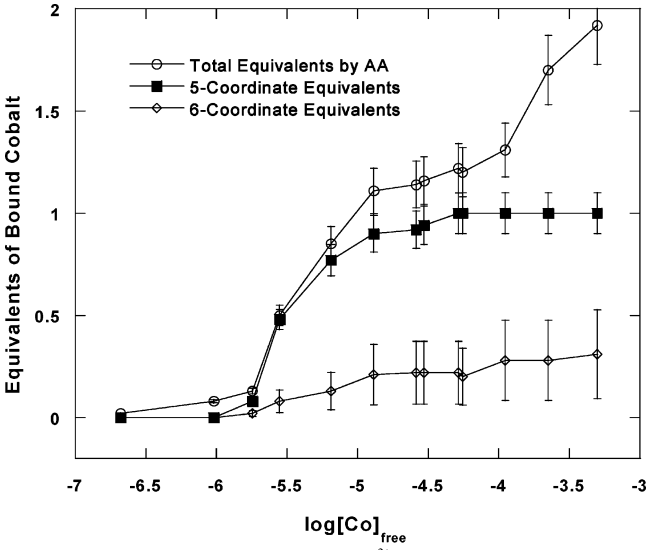

Figure 8. Anaerobic equilibrium dialysis of *Ec*MetAP versus Co^{2+}. [*Ec*MetAP] was initially 1.0 mM in 25 mM pH 7.5 HEPES with 150 mM KCl. After each addition of Co^{2+} to the dialysis buffer the dialysis was allowed to equilibrate. Then a sample was removed from the dialysis cassette and glycerol was added (1 part protein and 2 parts glycerol). After the MCD spectra were recorded, the total cobalt and protein concentrations were determined by AA and absorbance, respectively. The total number of equivalents of bound cobalt was determined as in Figure 6, but the 10-fold higher initial *Ec*MetAP concentration allowed for an extension in the range of [Co^{2+}]. The free cobalt concentration was calculated on the basis of the initial amount of cobalt added to the dialysis buffer and the dilution with glycerol. The numbers ofquivalents of 5-coordinate and 6-coordinate Co^{2+} were calculated using the MCD peak intensities (after Gaussian deconvolution) at 567 and 495 nm, respectively, and $\Delta\epsilon_{567}/\mathbf{H} = 1.9\ M^{-1}\ cm^{-1}\ T^{-1}$ and $\Delta\epsilon_{495}/\mathbf{H} = 17\ M^{-1}\ cm^{-1}\ T^{-1}$.

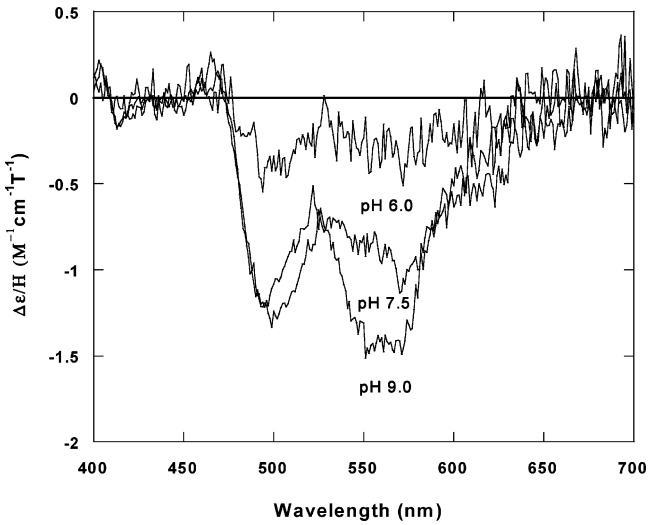

Figure 9. MCD spectra of *Ec*MetAP at pH 6.0 (MES), 7.5 (HEPES), and 9.0 (TRIS). All buffers were at 25 mM with 150 mM KCl. The samples were initially 1 mM in protein, and cobalt was introduced by anaerobic dialysis at 10 μM. After dilution with glycerol, the protein concentration was 0.33 mM and the free [Co^{2+}] was 3.3 μM. All spectra were recorded at 3.5 T and 1.6 K.

equivalents of bound 6-coordinate Co^{2+}. There is a third, adventitious, Co^{2+} binding site that has been reported in one crystal structure.[7] This site likely begins to bind cobalt at higher concentrations, so a sample of *Ec*MetAP dialyzed against 40 μM Co^{2+} was used for this calculation. This results in a value of $\Delta\epsilon_{495}/\mathbf{H} = 17 \pm 12\ M^{-1}\ cm^{-1}\ T^{-1}$. $\Delta\epsilon_{495}/\mathbf{H}$ and $\Delta\epsilon_{567}/\mathbf{H}$ are then used to determine the equivalents of 6- and 5-coordinate Co^{2+} in *Ec*MetAP through the whole range of free [Co^{2+}]. These are compared to the total bound cobalt as determined by AA in Figure 8.

A 1 mM sample of *Ec*MetAP was anaerobically dialyzed versus 0.5 mM Co^{2+} in 25 mM HEPES, 150 mM KCL, pH 7.5, for 48 h and then anaerobically dialyzed versus cobalt-free buffer for 96 h with a total of six buffer changes. This is somewhat analogous to the experiment shown in the lower right inset of Figure 6, but at 10 times higher MetAP concentration. At 48 and 96 h samples were removed and diluted with glycerol (1/3), and an MCD spectrum was taken. The MCD spectrum at 48 h was determined to have 0.24 ± 0.03 equiv of 5-coordinate Co^{2+} on the basis of the intensity of the 567 nm peak and 0.07 ± 0.04 equiv of 6-coordinate Co^{2+} on the basis of the intensity of the 495 nm peak. After 96 h of dialysis versus cobalt-free buffer, 0.11 ± 0.02 equiv of 5-coordinate Co^{2+} was found and 0.05 ± 0.04 equiv of 6-coordinate Co^{2+} was found. In the "level region" (Figure 8) where 1.1 equiv of Co^{2+} is bound to *Ec*MetAP (Figure 8, between 10 and 100 μM free Co^{2+}) the ratio of 6-coordinate to 5-coordinate Co^{2+} is 0.10. This ratio increases to 0.29 after 48 h of cobalt-free dialysis and further increases to 0.45 after 96 h of dialysis against cobalt-free buffer. Not all of the cobalt in the 48 and 96 h samples found by AA could be accounted for in the MCD spectra. Due to the large volumes of buffer that the protein samples were exposed to, a small amount of the bound cobalt had apparently oxidized to Co^{3+}, which is measured by AA but is MCD silent.

Effect of pH on Metal Binding. Figure 9 shows the effect of changing the pH on the MCD spectra of *Ec*MetAP when prepared by anaerobic dialysis against 10 μM Co^{2+}. The MCD spectrum of the pH 6.0 preparation shows that almost no 5- or 6-coordinate cobalt binds. This was confirmed by AA, which showed that only 0.12 equiv of cobalt was bound at pH 6.0. The pH 9.0 sample shows a dramatic change in the 495 to 567 nm peak intensity ratio, indicating that the relative amounts of 6-coordinate to 5-coordinate Co^{2+} are changing relative to those of the sample prepared at pH 7.5. It is seen that the amount of 6-coordinate Co^{2+} is nearly equal in both the pH 7.5 and 9.0 samples; however, the 5-coordinate Co^{2+}, as evidenced by the peak at 567 nm, is larger by 80%.

Since the pK_a values of the Glu and Asp side chain carboxylic acids are 4.4, these cannot be changing in degree of protonation from pH 6.0 to pH 9.0. However, the degree of protonation of the imidazole nitrogen of His 171 with a pK_a of 6.0 will change in this pH range. One might not expect a pH dependency of metal binding to a histidine imidazole because imidazole nitrogen is such a good transition-metal ligand; however, *Ec*MetAP is unusual in that the metal can be removed from the active site by dialysis against pure buffer. Thus, the Co^{2+} binding affinity dependence on pH supports the conclusion that the MCD peak at 567 nm is due to Co^{2+} with the imidazole nitrogen from His 171 as a ligand, which is the 5-coordinate Co(1) site shown in Figure 1. It is likely that the pK_a values in the active site of *Ec*MetAP are nearly those of the free amino acids since the site is hydrophilic. Furthermore, the fact that the MCD peaks at 495 and 567 nm have very different relative intensities at pH 7.5 and 9.0 is evidence that these are due to separate Co^{2+} species. Since the 6-coordinate Co^{2+} binding affinity is not enhanced when the pH is changed from 7.5 to 9.0, it must not have a histidine ligand, so the mixture of 6- and 5-coordinate

Co^{2+} is not due to equilibrium between the two coordination numbers on a cobalt atom in the same binding site. The mixture of 6- and 5-coordinate Co^{2+} arises from occupancy of two distinctly different binding sites such as Co(1) and Co(2) as shown in Figure 1. The simultaneous loss of 6- and 5-coordinate Co^{2+} binding affinity at pH 6.0 makes sense only if the small fraction of 6-coordinate Co^{2+} is a result of cooperative binding with the 5-coordinate Co^{2+}. This would account for the slope of 1.3 in the Hill plots.

Discussion

The electronic absorption spectrum, MCD spectra, AOMX calculations, equilibrium dialysis results, and pH study support previous reports that *Ec*MetAP binds nominally 1 equiv of Co^{2+} at the low concentrations of metal likely to be found in vivo.[15,17,21] Furthermore, we concur that the dominate Co^{2+} species is 5-coordinate and this cobalt is bound in the Co(1) site shown in Figure 1. However, our experiments show that there is a small fraction, approximately 10%, of 6-coordinate Co^{2+} that is also taken up by the enzyme at low metal concentrations. The ratio of 6-coordinate to 5-coordinate Co^{2+} remains constant until the 5-coordinate site saturates, at which point there is 1.1 equiv of cobalt bound/mol of enzyme. The Hill plots on equilibrium dialysis studies monitored by MCD or by AA yield slopes of $n = 1.3$, indicating a slight cooperative binding effect; thus, we conclude that, even at low concentrations of cobalt, there are a small fraction of binuclear sites. Further evidence of cooperative binding is provided by the loss of metal from both the 5- and 6-coordinate sites when the pH is lowered to 6.0. At this pH, the only protein ligand to Co(1) or Co(2) that will be significantly protonated is the imidazole nitrogen of His 171.

A dissociation constant of between 2.5 and 4.0 μM results if it is assumed that only a single cobalt binding site exists in the low concentration regime; however, this binding constant decreases to 0.25 μM if $n = 1.3$ and eq 3 is applied. In practice it is necessary to have 5 ± 2 μM Co^{2+} in the dialysis buffer to get 0.5 equiv of cobalt to bind to *Ec*MetAP, which is in the range of the dissociation constant determined by isothermal titration calorimetry[15b] but about 10-fold higher than that determined by activity titration.[15a] Our estimate for the K_d of the second cobalt is 0.2 ± 0.1 mM. This must be considered very tentative because we were unable to explore cobalt concentrations in the dialysis buffer above 1.6 mM due to protein aggregation. Furthermore, there is a third cobalt binding site identified in one of the crystal structures. The third metal binding site is on the outer edge of the enzyme and becomes at least partially occupied at cobalt concentrations near 1 mM.[7]

The Co^{2+} that binds to *Ec*MetAP is loosely bound. Most metalloenzymes, whether mono- or bimetallic, require some form of complexation agent to remove metals from the active sites. *Ec*MetAP is unusual in that dialysis against metal-free buffer is all that is required to remove most of the metal. This supports the hypothesis that *Ec*MetAP does not have a specific in vivo metal, but rather can enlist a variety of divalent metals depending on the environment.[3,19,20] The small fraction of bimetallic sites in *Ec*MetAP at low metal concentrations are more resistant to removal by dialysis against metal-free buffer than the monometallic 5-coordinate Co^{2+}. It is intriguing to speculate that these bimetallic sites may have a function in vivo. Studies are under way to determine what specific activity these sites may have separate from the major monometallic species.

The fit of the VTVH MCD 6-coordinate peak data in the low-temperature regime to a simple pseudo-Kramer doublet model rules out any strong magnetic coupling between the 6- and 5-coordinate Co^{2+}. This is consistent with the EPR results.[15a] Lack of strong coupling does not eliminate the possibility that Co(1) and Co(2) share bridging ligands, nor is there sufficient evidence from model complexes to infer whether the third bridging ligand in Figure 1 is hydroxide or water. Weak coupling between Co^{2+} ions in dimer complexes is the rule rather than the exception.[34−36] There are very few published studies in which the magnetic coupling constant, *J*, has been determined. Coupling in a series of $[Co_2(tren)_2X_2](BPh_4)_2$ complexes (X = oxalate/2, NCS^-, NCO^-, or N_3^-) was reported.[34] *J* was found to be -3.1 cm^{-1} for the oxalate, but $|J| < 0.5$ cm^{-1} for the other bridging ligands. In another series of Co(II) dimer complexes made with *N*,*N*,*N*-trimethyl-1,4,7-triazacyclononane and having a bridging unit of the type $Co_2(\mu\text{-OH})(\mu\text{-carboxylato})_2$ only high-temperature (98−298 K) magnetic susceptibility was measured, so no quantitative values for *J* were reported; however, the authors do state that coupling must be weak.[36] VTVH MCD is limited to detecting energy gaps of $0.5-1$ cm^{-1} and larger because the thermal energy, *kT*, at 1.5 K is about 1 cm^{-1}. On the basis of limited literature, this may be the range expected for a hydroxide (or aqua) bridged dimer.

One possible criticism of the MCD results is that the glycerol glassing agent and/or the low temperatures necessary to observe MCD somehow affect the active site or induce the formation of the small amount of 6-coordinate Co^{2+} that is observed. Countering these arguments are several observations: (1) the visible absorption spectrum of *Ec*MetAP with bound Co^{2+} is unaffected by added glycerol, (2) the JASCO spectropolarimeter generates an absorption spectrum simultaneously with the MCD spectrum (albeit a noisy spectrum compared to the MCD or RT spectrum generated on the Cary 6000i), and it has the same shape as the RT absorption spectrum, and (3) the equilibrium dialysis experiments conducted in pure buffer versus buffer with added glycerol yield the same dissociation constants and number of bound equivalents of cobalt (within error).

The large uncertainty in the estimate of $\Delta\epsilon_{495}/\mathbf{H}$ means that the fraction of 6-coordinate Co^{2+} (binuclear sites) could be as low as 3% or as high as 17%. Since the fraction of binuclear sites is minor, it is tempting to assume that they are not important for enzymatic activity. However, we cannot rule out the possibility that the binuclear sites are active to some yet unknown substrate, generally active, or even the only active form of the enzyme since the ratio of 6- to 5-coordinate Co^{2+} is invariant from the lowest metal concentrations at which *Ec*MetAP begins to bind cobalt. Lin et al. conducted a series of intriguing experiments on some wild-type and mutant *Ec*MetAP.[23] In the first experiment cobalt was omitted from the growth medium, and the isolated wild-type *Ec*MetAP was found to have a Co^{2+}/protein ratio of 1.6. In a second experiment *Ec*MetAP was produced from mutant *E. coli* in which Asp 97 (the bidentate carboxylate ligand to Co(2) in Figure 1) was replaced by an alanine. This mutant *Ec*MetAP contained no

(34) Duggan, D. M.; Hendrickson, D. N. *Inorg. Chem.* **1975**, *14*, 1944−1956.
(35) Lambert, S. L.; Hendrickson, D. N. *Inorg. Chem.* **1979**, *18*, 2683−2686.
(36) Chaudhuri, P.; Querbach, J.; Wieghardt, K.; Nuber, B.; Weiss, J. *J. Chem. Soc., Dalton Trans.* **1990**, 271−278.

cobalt. Furthermore, it was inactive even with added cobalt. One interpretation of this result is that this key ligand for Co(2) is missing so that no 6-coordinate Co^{2+} binds. We have noted that the specific activity of *Ec*MetAP increases until $[Co^{2+}] =$ 1 mM (using equilibrium dialysis) and then steeply drops as the cobalt concentration increases.[25] This is the region of $[Co^{2+}]$ at which the number of binuclear sites is rapidly increasing (Figure 8). It was reported by others that the specific activity reached a maximum with 1 equiv of Co^{2+} directly added to *Ec*MetAP and that no further increase in specific activity was noted up to 50 equiv of added Co^{2+} (which was 1 mM in Co^{2+}; [*Ec*MetAP] was 20 μM).[15a] These researchers propose that the negative pocket created by Asp 97 in the absence of Co(2) provides a binding site for the N-terminal amine substrate; thus, the mutant *Ec*MetAP missing Asp 97 cannot properly align substrates.[15a,b]

A recent study of the effect of pH changes on the activity of *Ec*MetAP reported a "bell-shaped" behavior from pH 6.0 to pH 8.5 with a maximum near pH 7.5.[15b] In the assay medium, $[Co^{2+}]$ was kept at 12 μM, very similar to the conditions at which we studied the pH effect on the MCD spectra (Figure 9). Changes in the molar absorptivity were noted with a minimum ϵ at pH 6.0 and maximum at pH 8.5. These spectral trends mirror our MCD results at low pH where the loss of MCD intensity is attributable to loss of bound metal. We propose that the activity loss at low pH is due to the release of the metal. The activity loss at high pH cannot be solely due to loss of bound metal since the MCD spectrum shows that more cobalt is bound at pH 9.0 than at pH 7.5 (at low metal concentrations). There is however a difference in the types of Co^{2+} that bind at pH 9.0. The amount of 6-coordinate Co^{2+} stays the same at pH 9.0, but the amount of 5-coordinate Co^{2+} increases by 80% compared to that at pH 7.5. Holz et al. attribute the loss of activity at higher pH to a water ligand on Co(1). The water serves as the nucleophile during turnover and is deprotonated (pK_a of 8.1) to hydroxide at pH 8.5.[15b] Loss of activity at the higher pH values could also be partly due to the limited solubility of free Co^{2+} since the K_{sp} of $Co(OH)_2$ is 2.5×10^{-16}. One of the reviewers has also pointed out that there are histidine residues near the active site that could also undergo changes with pH that affect activity. It is known, for example, that the inhibitor fumagillin covalently binds to His 79, a residue that is conserved in all structurally characterized MetAPs.[7] Active involvement of His 79 has been proposed in several mechanisms;[15b,22] thus, we must acknowledge that changes in His 79 with pH could also be responsible for activity loss.

Finally, we comment on the EXAFS study of *Ec*MetAP in light of our results.[17] The EXAFS study of *Ec*MetAP prepared with 1 equiv of bound cobalt did not detect the presence of a second metal. This we believe is not contradictory to our conclusion that there are a small number of bimetallic sites in *Ec*MetAP even when prepared at low metal concentration. Metal−metal scattering in EXAFS is weaker (1) for metals that are not directly bonded to one another, (2) for metals that are far apart (in *Ec*MetAP they are ca. 3.2 Å apart), and (3) when the metal has an imidazole nitrogen ligand.[37] These conditions are all met in *Ec*MetAP. Finally, the EXAFS fits were equally good to a 5-coordinate or 6-coordinate Co^{2+}.[17]

Acknowledgment. We gratefully acknowledge Professor W. Todd Lowther for kindly providing the stock culture of *E. coli.* We further acknowledge support from the Vermont Genetics Network through NIH Grant No. 1 P20 RR16462 from the BRIN program of the NCRR, the National Science Foundation, Award No. CHE-9708193, and the American Chemical Society/ Petroleum Research Fund, Award No. PRF 36424-B3.

JA0485006

(37) Scott, R. A. In *Physical Methods in Bioinorganic Chemistry*; Que, L., Ed.; University Science Books: Sausalito, CA, 2000; Chapter 9, p 498.